

## COMPARATIVE ANALYSIS OF STRUCTURE PERFORMANCE OF PDC CUTTER TOOTH SURFACE AND INTERFACE MATCHING PAIR

FUXIAO ZHANG, YANJUN LU

*School of Mechanical and Precision Instrument Engineering, Xi'an University of Technology, Xi'an, China*

*Corresponding author Fuxiao Zhang, e-mail: zhangfuxiaoswpu@163.com*

HAI ZHU, JUTONG DING

*Electromechanical Engineering College, Southwest Petroleum University, Chengdu, China*

With the improvement of research on the tooth surface and interface, the rock breaking technology of a polycrystalline diamond compact (PDC) bit has witnessed significant advancements and widespread applications in various domains. However, the current research on the tooth surface and interface is largely independent of each other, lacking integration between the two. This study aims to explore the influence of the connection between the tooth surface and interface on cutting efficiency and failure mechanisms during PDC bit cutting operations. Six different mating structures are selected for analysis, and the cutting process is simulated using Abaqus software in a consistent environment. The study examined the crushing specific energy, stress distribution, cutting force and temperature rise effect of different mating structures. Comparative analysis revealed that the efficiency and failure mechanism of the cutter are influenced by the interface shape, both within the same tooth shape and across different tooth shapes. Among the selected mating structures, the saddle-tooth surface with a radial interface exhibited superior performance in all aspects and demonstrated significant improvements. The findings provide a theoretical foundation for the study of the mechanism behind PDC cutter mating structures.

*Keywords:* Abaqus, PDC cutter, interface structure, matching pair

### 1. Introduction

The polycrystalline diamond compact (PDC) cutter plays a crucial role in the cutting process of PDC bits, with its performance significantly influencing the drilling effectiveness. In recent years, the drilling industry has witnessed the emergence of numerous specialised tooth profiles, owing to continuous advancements in PDC tooth profile research and development. Alongside improvements in cutter profile and interface optimisation, the drilling technology has made a remarkable progress, leading to enhanced drilling efficiency. With its extensive adaptability to various formations and cost-effectiveness, PDC bits have captured more than 70% of the market share (Zhang *et al.*, 2022). The global trend of ultra-deep drilling has further solidified the use of PDC bits as the mainstream approach for efficient and rational resource extraction (Zhu *et al.*, 2021).

To comprehensively understand the action mechanisms of PDC cutters, researchers worldwide have conducted studies on the rock breaking mechanism of PDC bits, predominantly employing empirical models and finite element simulations. Liu *et al.* (2018) analysed the rock breaking process of cutting tools using discrete elements. Fu *et al.* (2022) employed discrete element analysis to analyse PDC cutting forces, studying the force response of rock in conjunction with microscopic failure mechanisms and elucidating the influence of tool geometry. Wu *et al.* (2020) utilised the finite element method to simulate rock breaking and proposed a novel simulation method for optimising PDC rock breaking research. Hang *et al.* (2013) deserved recognition

for their ability to simultaneously reproduce elastoplastic strain, damage and brittle fracture, which they employed in the study of tool-rock interaction, among other applications. With the maturation of finite element simulation technology and improvement in analysis methods, the use of finite element simulation software for analysis purposes has become a prevailing trend in PDC rock breaking analysis.

To investigate potential connections between different tooth surfaces and interfaces of PDC cutters, a comparative study is conducted on the structural performance of three distinct tooth surfaces and their corresponding interfaces and interface matching pairs. Interfaces with favourable performance are selected for analysis. A PDC cutter linear cutting rock model is constructed using Abaqus to simulate PDC cutter cutting tests, and the influence of accessory structure on the cutting action is examined from four perspectives: the crushing specific energy, cutting force, cutter stress and temperature rise effect.

## 2. Interface structure optimisation

The interface plays a crucial role in determining the overall cutting performance of a PDC bit. Thermal residual stress in PDC is widely considered the primary cause of abnormal failures. Different forms of interface structures and variations in material thickness within the same material can significantly influence the size and distribution of thermal stress (Xu, 2009). This study focuses on optimising the four interface structures depicted in Fig. 1.

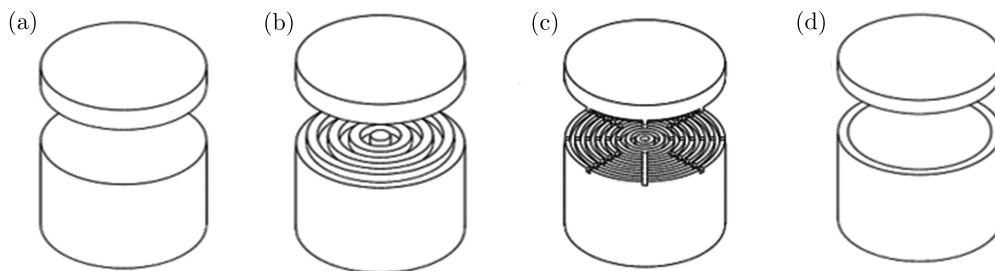


Fig. 1. Four different interface structures: (a) flat interface, (b) circular ring interface, (c) radial interface, (d) circular and concave interface

Abaqus/Standard is used to simulate the cooling process of a synthetic cavity, reducing the residual stress generated inside the cutter from 1000°C to 25°C. The materials used are listed in Table 1, and the mesh is created using the transition mesh drawing method and an adaptive mesh algorithm.

**Table 1.** Parameters of the cutter and rock material

Material	Modulus of elasticity [GPa]	Density [Kg/m <sup>3</sup> ]	Thermal conductivity [J/(ms°C)]	Specific heat capacity [J/(Kg°C)]	Coefficient of thermal expansion [10 <sup>-6</sup> /°C]	Poisson's ratio [-]
PCD	890	3510	543	790	2.5	0.07
Hard alloy	579	15000	100	230	5.2	0.22
Rock	40	2650	3.5	800	52	0.25

Figure 2 displays the resulting equivalent residual stress nephogram for the output interface.

The analysis results shown in Fig. 2 reveal that the flat interface (a) exhibits the most regular stress distribution with the smallest equivalent stress value. The equivalent stress gradually increases from the centre to the circumference of the cemented carbide layer interface, resulting in stress concentration at the outer circumference of the matrix interface of the flat interface teeth.

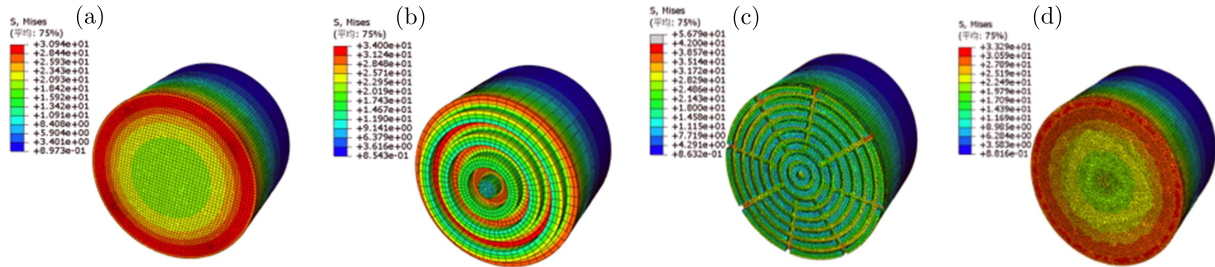


Fig. 2. Equivalent stress nephogram of four interfaces: (a) flat interface, (b) circular ring interface, (c) radial interface, (d) circular and concave interface

The circular concave interface (d) shares similarities with the flat interface, but the equivalent stress of the cemented carbide layer interface is slightly higher, leading to more severe stress concentration at the matrix interface. The circular interface (b) demonstrates significant stress concentration at the interface, particularly in the areas that match its geometric characteristics. On the other hand, the radial interfacial tooth (c) exhibits a more balanced distribution of the equivalent stress on its surface due to its interface joint being divided into multiple surfaces by multiple rings and transverse stiffening bars, thereby avoiding significant stress concentration.

To further evaluate the special-shaped interface, the circumscribed equivalent residual stress on the working surface of the PCD layer is extracted (Fig. 3), and its distribution along the circumferential path is plotted (Fig. 4).

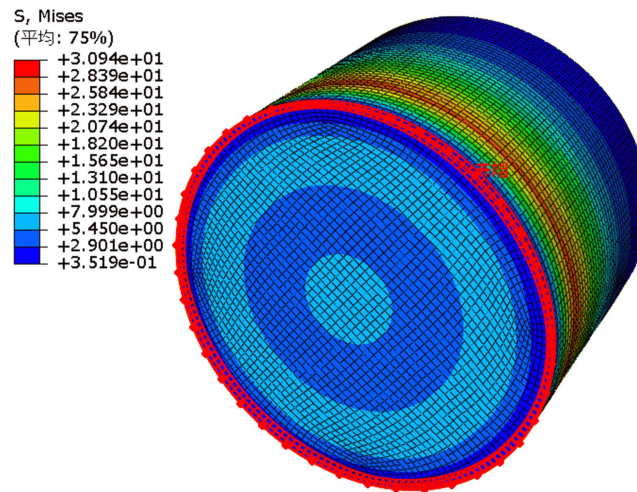


Fig. 3. Stress extraction of the working surface

The distribution of the equivalent residual stress along the circumference of the working surface of the cutter corresponds to geometric characteristics of the interface. The plane interface, radial interface, concave interface and circular interface exhibit a uniform stress distribution. The circular interface experiences a notably higher stress value, whereas the flat interface demonstrates lower stress. Overall, the plane, radial, round and concave interfaces exhibit better performance.

From Fig. 5 one can see that the plane interface, circular interface and radial interface still perform the best, with values of 1.42 MPa, 1.53 MPa and 1.52 MPa, respectively. These values are significantly reduced compared with the circular interface. In summary, among the examined samples, the radial interface exhibits the most favourable effect. The equivalent residual stress distribution and surface stress at the interface joint are relatively uniform, avoiding significant stress concentration, and resulting in a low average equivalent residual stress. Therefore, the

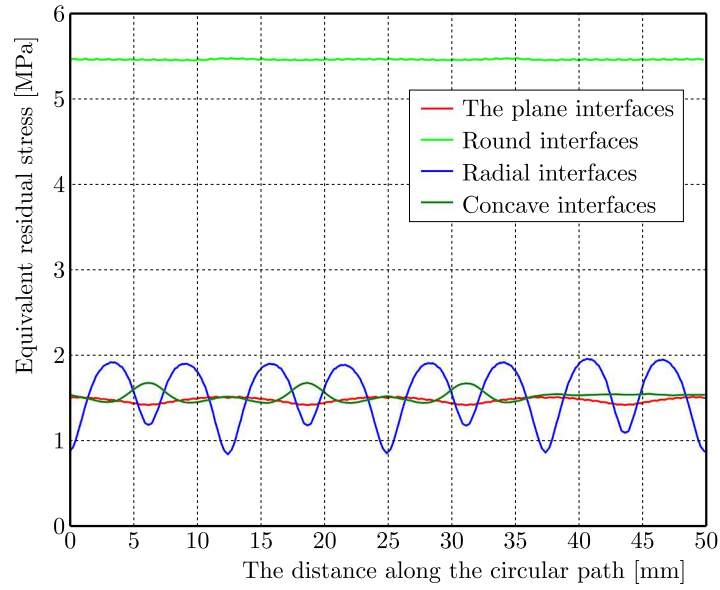


Fig. 4. Circumferential equivalent residual stress on the working surface

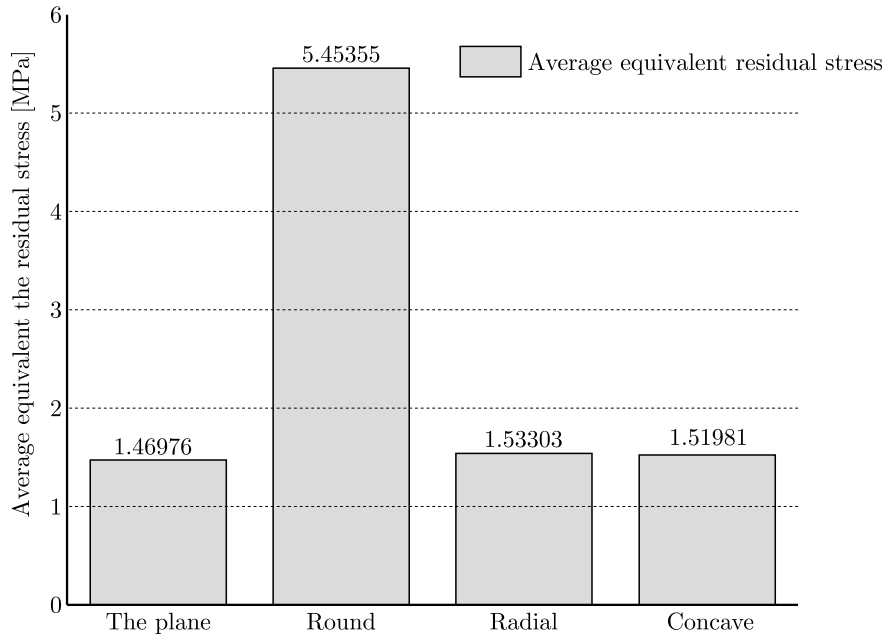


Fig. 5. Average residual stress at the four interfaces

radial interface is selected as the mating structure interface, with the flat interface serving as a comparison object for a comprehensive study on the performance of the mating structure.

### 3. Establishment of the finite element model of auxiliary structures

Six different tooth surfaces and interface auxiliary structures have been established, as depicted in Fig. 6. The size of the rock model is  $50 \times 30 \times 15$ , whereas the PDC cutter size is  $15.88 \times 13.2$  (unit: mm).

The rock employs the Drucker-Prager model with a fracture displacement set at 0.001. The material parameters of the rock and cutter are listed in Table 1 (Yang *et al.*, 2007; Lu *et al.*, 2004; Liang, 2005). The dynamic process of the PDC teeth cutting rock is solved using

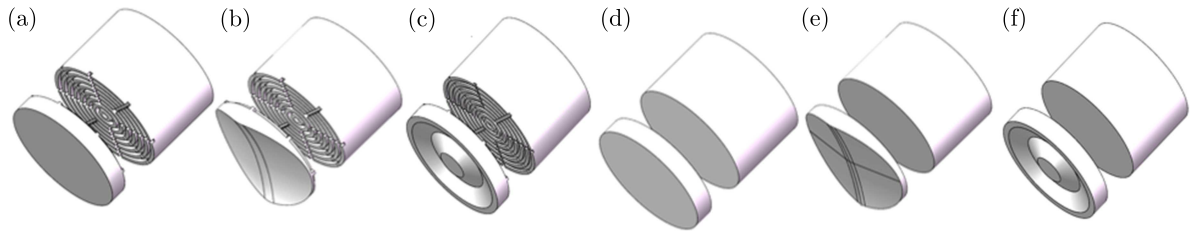


Fig. 6. Schematic of six different auxiliary structures: (a) plane tooth-radial interface, (b) saddle tooth-radial interface, (c) multidimensional cutter tooth-radial interface, (d) plane-tooth interface, (e) saddle tooth-flat interface, (f) multidimensional cutter tooth-panel interface

Abaqus/Explicit. The analysis step time is 0.01 s, and the analysis step follows the “power, temperature-displacement, display” sequence (Zhu, 2015).

## 4. Comparative analysis of simulation results

### 4.1. Evaluation index

The evaluation of different auxiliary structures in this comparative analysis is based on several key factors that influence the performance of the cutter. These factors include stress fluctuation, which serves as an objective indicator for cutter lifespan, quantitative measurement of rock breaking efficiency through crushing specific work, measurement of the tooth impact degree through cutting force fluctuation and analysis of the temperature rise curve and tooth profile contact surface stress fluctuation. To account for any deviation resulting from the simulation model, several groups of grids with different quantities were added and re-run to verify grid independence. The following results confirmed the grid independence, with errors kept within 5%.

In summary, the performance evaluation criteria for each tooth profile are as follows: crushing specific work, cutting force fluctuation, temperature rise curve and tooth profile contact surface stress fluctuation.

### 4.2. Influence of the auxiliary structure on specific work of crushing

In the oil drilling industry, the evaluation of rock breaking efficiency is based on the energy required for toothed rock breakage, known as the specific energy of crushing. Zhou *et al.* (2017) indicated that the specific energy of crushing, which represents the energy consumed per unit volume of rock, could quantitatively reflect the rock breaking efficiency. It can be approximated as

$$MSE_n \approx \frac{A}{V_c} \quad (4.1)$$

Among them,  $MSE_n$  stands for the crushing specific work,  $A$  is the energy consumed by breaking a certain volume of rock,  $V_c$  is the volume of broken rock (Teale, 1965).

The shape of the tooth surface determines the cutting path of the rock. When comparing tooth shapes with the same relative contact area, the volume of rock cut per unit time is approximately the same. However, the contact area of the saddle-shaped tooth is smaller relative to the projection plane, resulting in a different cutting trajectory compared with the other two tooth shapes (Figs. 7b and 7e).

Taking the crushing power as a priority for cutting performance allows for an objective reflection of the rock breaking efficiency of the bit. The final cutting diagrams in Fig. 7 show that the volume difference of toothed rocks with the same relative contact area is small, with

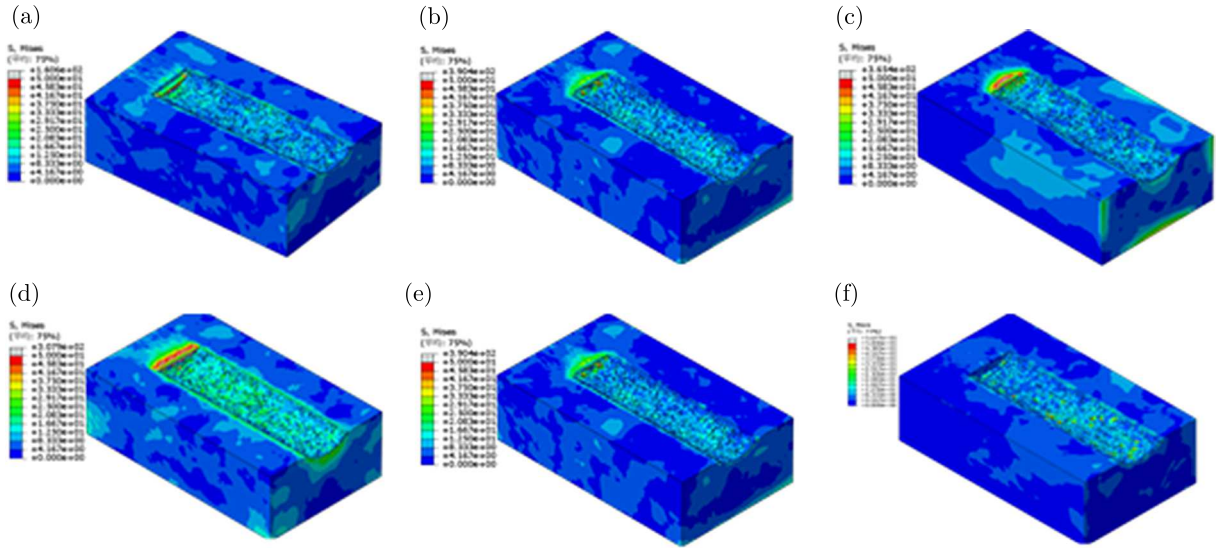


Fig. 7. Cut marks of rock: (a) plane tooth-radial interface, (b) saddle tooth-radial interface, (c) multidimensional cutter tooth-radial interface, (d) plane-tooth interface, (e) saddle tooth-flat interface, (f) multidimensional cutter tooth-plane interface

any differences falling within the error range due to mesh failure during different simulation processes. The initial unstable trend observed in the front section of each model necessitates the removal of data from that region to ensure data accuracy. Despite differences in the correction points among different auxiliary structures, their impact on the overall specific energy of crushing can be ignored.

As shown in Table 2, when using a flat interface, the specific energy of crushing shows a small difference among various tooth shapes. The maximum specific energy of crushing is 11.86 for planar teeth, whereas the minimum is 11.2 for multidimensional cutters. When the same tooth shape is used, the difference in specific energy of crushing is noticeable with changes in the interface. The most significant difference is observed with the saddle structure, which reduces the specific energy of crushing by 14%. When the tooth surface and interface are combined to form a mating structure, the saddle-shaped pairing structure (saddle-tooth interface) demonstrates an obvious improvement compared with the flat tooth-flat interface effect.

**Table 2.** Work done by external forces, volume variation of rock and crushing specific work of cutting pairs

Auxiliary structure		Work done by external forces [mJ]	Volume change of rock [mm <sup>3</sup> ]	Specific work of crushing [mJ/mm <sup>3</sup> ]
Flat interface	Planar tooth	8725.655	735.5	11.86357
	Saddle tooth	7246.007	628.0	11.53823
	Multidimensional cutter	7850.786	701.5	11.19143
Radial interface	Planar tooth	7446.651	717.8	10.37427
	Saddle tooth	6196.092	623.0	9.945572
	Multidimensional cutter	7748.145	694.6	11.15483

#### 4.3. Influence on tooth stress during cutting of the mating structure

The maximum stress fluctuation on the main contact surface of different teeth reflects stress fluctuations at the contact point between the cutter and rock to a certain extent, indicating

periodic changes in the stress (Beak *et al.*, 2017). The average stress can provide insight into the stress of the contact surface, but it has a low impact on the tooth life. Therefore, the maximum stress fluctuation is used as the basis for assessing quality of the tooth.

During the simulation of cutting actions for each mating structure, the stress fluctuation on the cutter exhibits a pulsating distribution and instability due to dynamic calculation in Abaqus. To facilitate a more intuitive comparison, the maximum stress is limited to a range of 100 MPa in the displayed maps. It is observed that the stress is mainly concentrated on the contact surface between the tooth and rock, with the stress distributed in a specific area of the tooth. Figure 8 illustrates a comparison of stress regions and stress fluctuations on the main contact surface of the (a) plane tooth-radial interface tooth shapes.

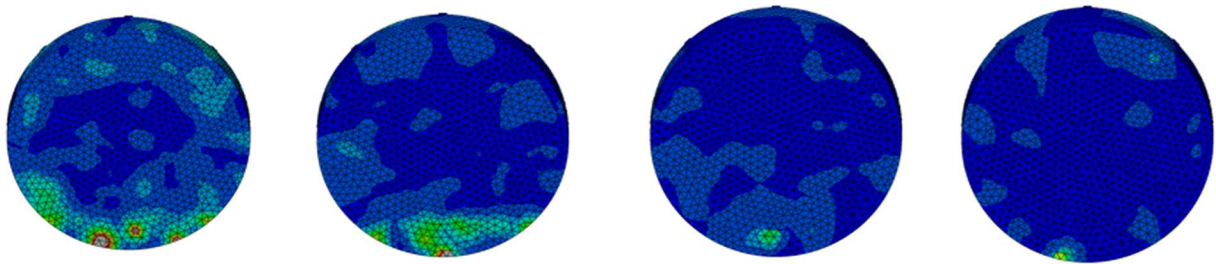


Fig. 8. Tooth surface stress fluctuation diagram of the mating structure

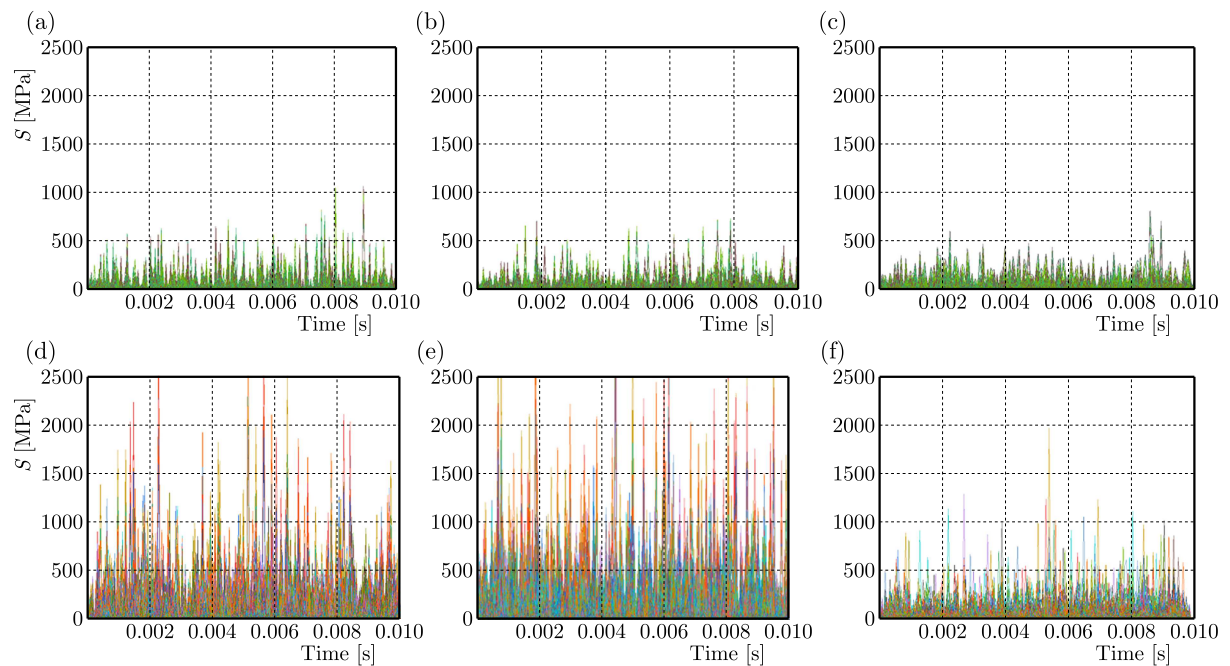


Fig. 9. Comparison diagram of the main contact stress of each pair: (a) planar tooth-radial interface, (b) flat interface-tangential force, (c) multidimensional-radial interface, (d) planar tooth-flat interface, (e) saddle tooth-flat interface, (f) multidimensional-flat interface

As shown in Fig. 8, optimisation of the interface structure significantly improves the stress distribution and magnitude on the tooth surface. To analyse the stress data, a clear standard for measuring the stress fluctuation during dynamic calculation is currently lacking. Zhang *et al.* (2019) sampled 8 points to observe stress, but it is not applicable when there is a significant stress fluctuation. To address this, a new comparison method is introduced here. It involves sampling of the main contact area, dividing it into 1500 sampling points and exporting the sampling point data for analysis. As each sampling point has 200 time segments, the stress fluctuation

on the tooth surface can be analysed more intuitively. Although this method requires a large amount of data and slower derivation, it provides more accurate analysis results. In this study, the main stress distribution points in the main contact area of each auxiliary structure model were selected, and the corresponding equivalent stress values for each distribution point in each time period were derived and analysed (Fig. 9).

To better illustrate the data, separate analyses of the maximum values in each segment were conducted for the above mating structures to represent the volatility (Fig. 10).

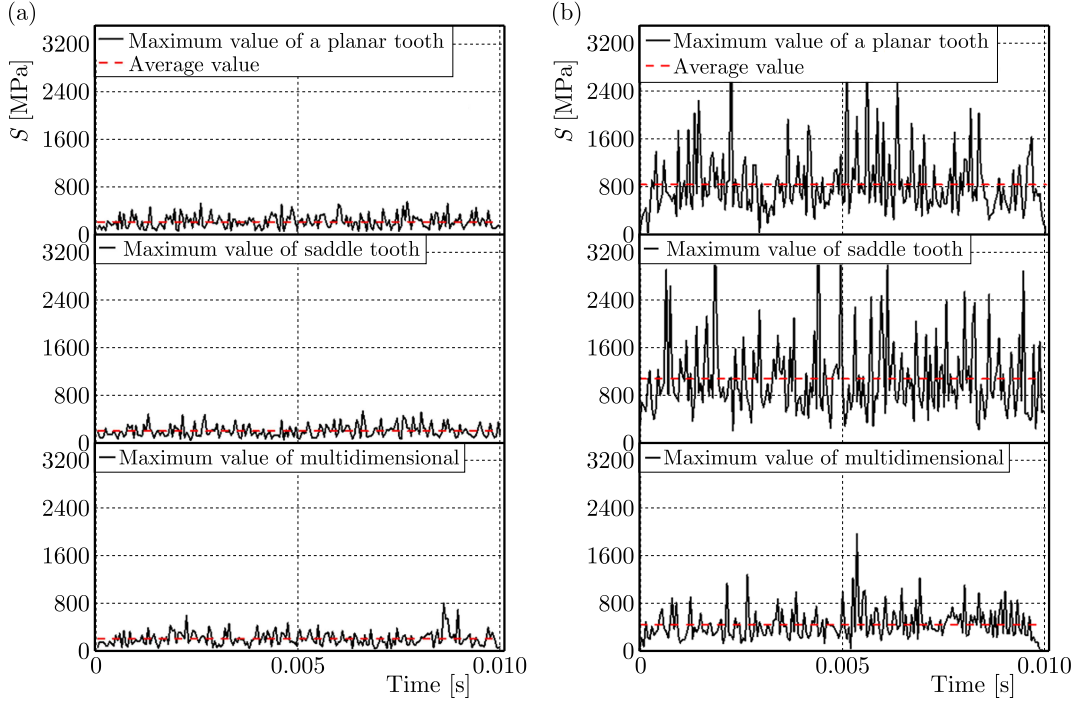


Fig. 10. Maximum value and average value of each auxiliary structure in each period

By comparing the mating structures between the flat interface (a) and the radial interface (b), it is evident that the use of the radial structure can significantly reduce the maximum stress and average stress on the three tooth surfaces (Baker, 2021).

As shown in Fig. 11, when the radial interface is used, the stress reduction on saddle teeth is most pronounced. The average stress value for saddle teeth with a flat interface is 1076.79 MPa, whereas it decreases to 191.35 MPa with the radial interface, which is 5.6 times lower. Additionally, when the plane interface is used, the stress on multidimensional teeth is significantly reduced compared with planar and saddle teeth. These results indicate that the radial interface effectively enhances the resistance of the tooth surface to macroscopic fracturing. When a flat interface is used, the multidimensional cutter demonstrates a distinct advantage, which is consistent with the actual performance of the multidimensional cutter.

#### 4.4. Influence of the coupling structure on the cutting force

In addition to the specific work and stress factors, the instantaneous reaction cutting force and its fluctuation greatly affect the life of the cutter. Therefore, the impact load on the tooth in the rock breaking process can be measured by the size and fluctuation of the cutting force (Lin., 2019; Zhang *et al.*, 2021). Theoretically, a smaller fluctuation of the cutting force is better as it helps extending the life of the cutter.

The instantaneous tangential and axial forces at the radial interface and interface are compared and analysed. For the tangential force, as shown in Fig. 12, the instantaneous tangential

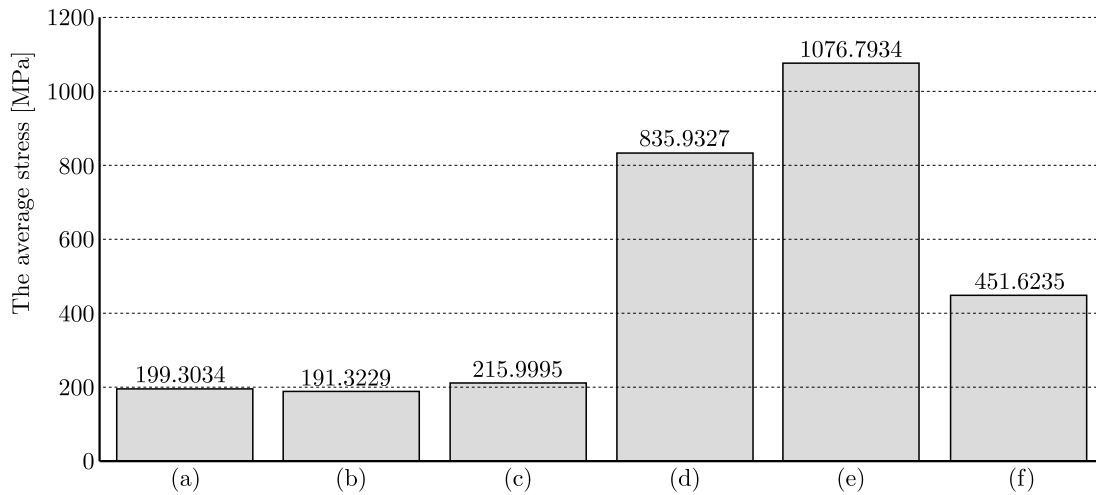


Fig. 11. Average stress of the auxiliary structure: (a) planar tooth-radial interface, (b) flat interface-tangential force, (c) multidimensional-radial interface, (d) planar tooth-flat interface, (e) saddle tooth-flat interface, (f) multidimensional-flat interface

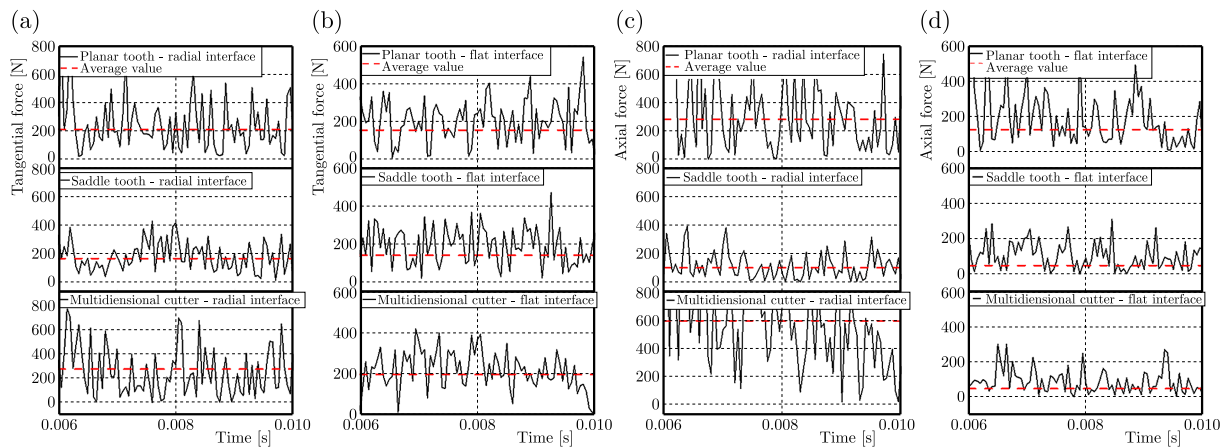


Fig. 12. Instantaneous tangential force and axial force comparison: (a) radial interface-tangential force, (b) flat interface-tangential force, (c) radial interface-axial force, (d) flat interface-axial force

force fluctuation does not change significantly due to the interface, except for the saddle-toothed radial interface. However, the tangential force magnitude and fluctuation increased. The tangential force represents the ease of rock breaking for cutters, where a smaller tangential force indicates easier rock destruction. Whether the radial interface (a) or the flat interface (b) is used, the tangential force of the saddle structure is smaller and more stable than that of other auxiliary structures.

The axial force represents the weight on the bit required by a single tooth. As shown in Fig. 12, compared with the flat interface (d), both multidimensional cutters and planar teeth using the radial interface (a) will increase the axial cutting force and fluctuation. This effect is most significant on multidimensional cutters. The instantaneous axial cutting force and fluctuation of saddle teeth exhibit little change. From the average level of the tangential and axial force, as shown in Table 3, when the radial interface is used, the average tangential force of plane teeth remains almost unchanged, whereas for saddle-shaped teeth decrease and for multidimensional cutters increase significantly. Additionally, the radial interface significantly increases the axial force level of the tooth shape, with the multidimensional cutter showing the most significant increase (6.8 times), followed by the plane teeth (1.6 times). The influence on saddle teeth is low.

**Table 3.** Anisotropic values of the average cutting force of each pair structure

Interface shape	Tooth surface shape	Mean value of tangential force [N]	Mean value of axial force [N]
Radial	Planar tooth	206	285
	Saddle tooth	166	101
	Multidimensional cutter tooth	248	594
Plane	Planar tooth	203	181
	Saddle tooth	188	89
	Multidimensional cutter tooth	195	88

In sum, the radial interface structure significantly decreases the tangential force of saddle teeth, but the axial force changes little. Planar and multidimensional cutters show improvements, with multidimensional cutters exhibiting the most noticeable changes. The saddle-radial interface coupling structure demonstrates excellent performance in both the axial and tangential forces, with a lower degree of cutting force fluctuation. This indicates that PDC bits using a saddle-shaped coupling structure not only require less torque but also have stronger axial intrusion ability, smoother cutting ability and are less prone to tooth damage caused by alternating loads. Therefore, when evaluating the cutting force, the radial interface is used for lifting saddle teeth, whereas the multidimensional cutters will be subjected to the radial interface reaction.

#### 4.5. Influence of the accessory structure on the temperature rise effect

During downhole operations, the diamond mesa experiences high tensile stress after the temperature rises. Simultaneously, the cooling effect of the drilling fluid results in different contraction between the diamond layer and carbide matrix, accelerating crack propagation (Gao *et al.*, 2019). Hence, the temperature rise curve is considered a standard to measure the quality of teeth.

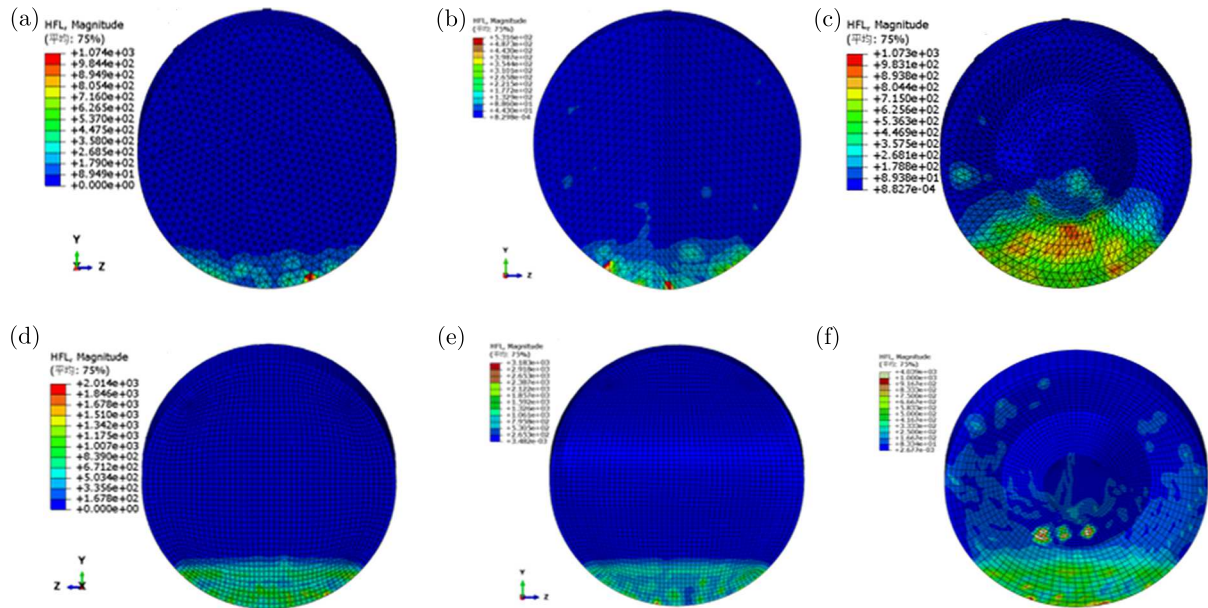


Fig. 13. Heat flow vector of each auxiliary structure: (a) plane tooth-radial interface, (b) saddle tooth-radial interface, (c) multidimensional tooth-radial interface, (d) plane tooth-plane interface, (e) saddle tooth-plane interface, (f) multidimensional tooth-plane interface

The heat generated on the tooth surface varies with different accessory structures. In this paper, the heat flow vector is introduced to simulate heat conduction. As shown in Fig. 13b and 13e, the magnitude of the radial vector heat flow is significantly reduced compared with the flat interface. Among the auxiliary structures, the saddle-toothed interface auxiliary structure exhibits the lowest heat generation, indicating better performance in heat conduction and reduced heat generation.

Owing to the differences in the heat flow vector of each coupling structure, it will certainly affect the surface temperature of PDC cutters (Grimmert *et al.*, 2019). During the initial cutting stage, when the front face of the cutter comes into contact with the rock, high-speed friction and extrusion between the teeth and the rock surface lead to rapid heat accumulation. After reaching a certain stability, the temperature remains within a certain range. On the other hand, a low temperature fluctuation also reduces the likelihood of PDC delamination caused by an uneven coefficient of thermal expansion inside the diamond (Hareland *et al.*, 2009). As seen in the derived chart from Abaqus, the temperature changes of the selected unit nodes in each model are too intensive, and the change trend is minimal. Therefore, the temperature rise curve is introduced, taking the average value of each unit node in each time period, which allows for a more intuitive comparison of temperature differences between the results of each coupling structure. Figure 14a displays the temperature rise curve of each model, where all auxiliary structures, except for the saddle-tooth interface, are influenced by the high-speed heat accumulation during the early stage.

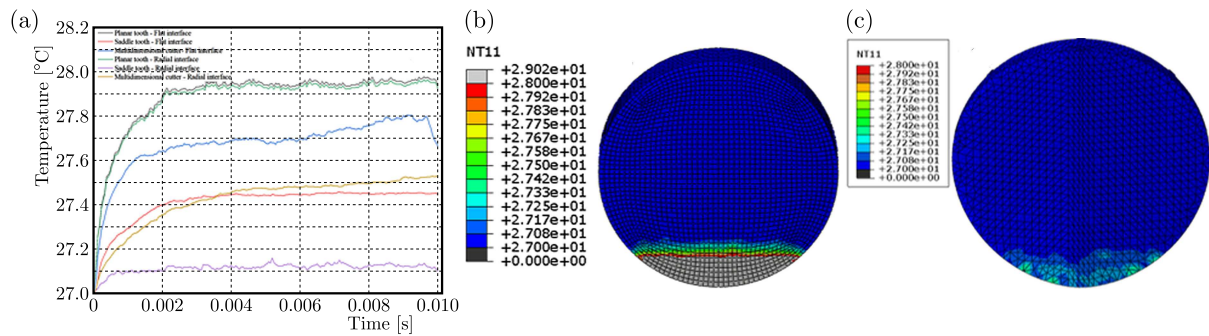


Fig. 14. Tooth surface temperature contrast: (a) temperature rise curve of each auxiliary tooth profile, (b) plane tooth-plane interface, (c) saddle tooth-radial interface

From the temperature rise curve of the auxiliary structures, the temperature rise tends to decrease when the radial interface structure is used, especially in the case of the saddle-tooth and the radial interface auxiliary structure (Fig. 14b and 14c). Furthermore, when the interface is the same, the tooth shape is also a contributing factor to the noticeable difference in the temperature rise curve, with saddle-shaped teeth exhibiting the lowest temperature rise effect.

## 5. Conclusion

In this paper, the optimization of the cutting tooth interface and the tooth surface and interface matching structure were studied. The main conclusions are summarized as follows.

- The comparative analysis of different interfaces with the same tooth shape reveals that different interfaces have a significant influence on the overall performance of the cutter. The radial interface needs to be paired with a specific tooth shape to achieve optimal performance, with the strongest reaction observed in multidimensional cutting teeth when using the radial interface.

- The comparison of different tooth shapes at the same interface demonstrates that different tooth shapes have varying influences on the crushing specific work, cutting force, stress distribution and temperature rise effect of PDC teeth. When using flat tooth shapes, PDC teeth should be selected based on the specific application. In the case of the flat interface, multidimensional cutters exhibit lower stress fluctuations and crushing specific work compared with other tooth shapes, making them a better choice for overall cutting performance.
- The comparative analysis of each coupling structure highlights the saddle-tooth radial interface as a suitable choice for evaluating the crushing specific work, cutting force, stress distribution and temperature rise effect.

#### *Acknowledgements*

This work was supported by the National Natural Science Foundation of China (Grant No. 52075438), the Key Research and Development Program of Shaanxi Province of China (Grant No. 2020GY-106), and the Open Research Fund of Key Laboratory of Oil & Gas Equipment of Ministry of Education (Grant No. OGE201702-110).

#### References

1. BAEK M.-S., PARK H.S., LEE J.-I., LEE K.-A., 2017, Effect of diamond particle size on the microstructure and wear property of high pressure high temperature (HPHT) sintered polycrystalline diamond compact (PDC), *The Korean Institute of Metals and Materials*, **55**, 790-797
2. BAKER H., 2021, *StayCool 2.0 Multidimensional Cutter Technology [EB/OL]*, <https://dam.bakerhughes.com/m/7edd5c3a7cb78480/original/StayCool-2-0-Multidimensional-Cutter-Technology-Overview-PDF>
3. FU Z., TERGEIST M., KUECK A., OSTERMEYER G.P., 2022, Investigation of the cutting force response to a PDC cutter in rock using the discrete element method, *Journal of Petroleum Science and Engineering*, **213**
4. GAO M.Y., ZHANG K., ZHOU Q., *et al.*, 2019, Research on PDC high speed rock cutting mechanism based on Abaqus, *China Petroleum Machinery*, **47**, 1-7
5. GRIMMERT A., PACHNEK F., WIEDERKEHR P., 2023, Temperature modeling of creep-feed grinding processes for nickel-based superalloys with variable heat flux distribution, *CIRP Journal of Manufacturing Science and Technology*, **41**, 477-489
6. HARELAND G., NYGAARD R., YAN W., WISE J.L., 2009, Cutting efficiency of a single PDC cutter on hard rock, *Journal of Canadian Petroleum Technology*, **48**, 6, 60-65
7. HUANG H., LECAMPION B., DETOURNAY E., 2013, Discrete element modeling of tool-rock interaction I: rock cutting, *International Journal for Numerical and Analytical Methods in Geomechanics*, **37**, 1913-1929
8. LIANG Z., 2005, *Analysis of Rock Failure Process in Three-Dimensional Condition and Study on its Numerical Test Method*, Northeast University
9. LIN Z., 2019, *Research and Design of New Non-Planar PDC Cutting Gear*, Southwest Petroleum University
10. LIU W.J., ZHU X.H., LI B., 2018, The rock breaking mechanism analysis of rotary percussive cutting by single PDC cutter, *Arabian Journal of Geosciences*, **11**, 192
11. LU Y., GE X., JIANG Y., *et al.*, 2004, Full-process tests and constitutive equations of conventional triaxial compression in marble, *Journal of Rock Mechanics and Engineering*, **23**, 2489-2493
12. TEALE R., 1965, The concept of specific energy in rock drilling, *International Journal of Rock Mechanics and Mining Sciences and Geomechanics Abstracts*, **2**, 57-73

13. WU Z.B., ZHANG S., WANG Y.Y., *et al.*, 2020, Parameterized tooth distribution and rock breaking simulation of PDC bit based on Abaqus, *Petroleum Machinery*, **483**, 30-36
14. XU G., 2009, *Study on Thermal Residual Stress and Interface Structure Optimization of PDC for Oil Field Drilling*, Central South University
15. YANG T., XU C., WANG B., *et al.*, 2007, Cohesion and internal friction angle in triaxial tests of rock and soil, *China Mining*, **12**, 104-107
16. ZHANG F., LU Y., XIE D., LUO H., SHI R., ZHANG P., 2022, Experimental study on the impact resistance of interface structure to PDC cutting tooth, *Engineering Failure Analysis*, **140**
17. ZHANG Z., ZHAO D., ZHAU Y., XHOU Y., TANG Q., HAN J., 2019, Simulation and experimental study on temperature and stress field of full-sized PDC bits in rock breaking process, *Journal of Petroleum Science and Engineering*, **186**, 1, 106679
18. ZHANG Z., ZHAO D., ZHAO Y., GAO K., ZHANG C., LÜ X., 2021, 3D numerical simulation study of rock breaking of the wavy PDC cutter and field verification, *Journal of Petroleum Science and Engineering*, **203**, 108578
19. ZHOU Y., ZHANG W., GAMWO I., LIN J.-S., 2017, Mechanical specific energy versus depth of cut in rock cutting and drilling, *International Journal of Rock Mechanics and Mining Sciences*, **100**, 287-297
20. ZHU X., LUO Y., LIU W., YANG F., LI Z., LU D., 2021, Rock cutting mechanism of special-shaped PDC cutter in heterogeneous granite formation, *Journal of Petroleum Science and Engineering*, **210**, 3, 110020
21. ZHU Y., 2015, Research on explicit dynamical analysis method based on Abaqus, *Mechanical Design and Manufacturing*, **4**, 107-109

*Manuscript received July 18, 2023; accepted for print September 17, 2023*